

Full length article

# Statistical mechanics of normal grain growth in one dimension: A partial integro-differential equation model



Felix S.L. Ng

Department of Geography, University of Sheffield, Winter Street, Sheffield S10 2TN, UK

## ARTICLE INFO

## Article history:

Received 5 May 2016

Received in revised form

12 August 2016

Accepted 15 August 2016

## Keywords:

Grain growth

Mean-field model

Statistical mechanics

Coarsening dynamics

## ABSTRACT

We develop a statistical-mechanical model of one-dimensional normal grain growth that does not require any drift-velocity parameterization for grain size, such as used in the continuity equation of traditional mean-field theories. The model tracks the population by considering grain sizes in neighbour pairs; the probability of a pair having neighbours of certain sizes is determined by the size-frequency distribution of all pairs. Accordingly, the evolution obeys a partial integro-differential equation (PIDE) over ‘grain size versus neighbour grain size’ space, so that the grain-size distribution is a projection of the PIDE’s solution. This model, which is applicable before as well as after statistically self-similar grain growth has been reached, shows that the traditional continuity equation is invalid outside this state. During statistically self-similar growth, the PIDE correctly predicts the coarsening rate, invariant grain-size distribution and spatial grain size correlations observed in direct simulations. The PIDE is then reducible to the standard continuity equation, and we derive an explicit expression for the drift velocity. It should be possible to formulate similar parameterization-free models of normal grain growth in two and three dimensions.

© 2016 Acta Materialia Inc. Published by Elsevier Ltd. This is an open access article under the CC BY license (<http://creativecommons.org/licenses/by/4.0/>).

## 1. Introduction

Normal grain growth (NGG) refers to the gradual increase of the mean grain or crystal size  $\bar{x}$  of a polycrystalline material, as grain-boundary motion causes larger grains to consume smaller grains and small grains to be eliminated. For over five decades, NGG has been studied as a fundamental process affecting texture evolution in metals and geological materials [1,2], and more broadly in connection with coarsening dynamics (e.g. soap-bubble growth) in various physical, social and biological systems; e.g. [3–6]. It is observed that, at large time  $t$ , NGG obeys the growth law

$$\bar{x} \sim (Ct)^m \quad (1)$$

(where the grain-growth exponent  $m$  and bulk growth rate  $C$  are positive constants), with the frequency distribution  $n(x, t)$  of the grain size  $x$  tending to a statistically quasi-stationary, or ‘invariant’, self-similar state. For NGG in two- and three-dimensional (2D and 3D) polycrystals with uniform grain boundaries, whose migration rate is curvature-driven, a parabolic growth law with  $m = 1/2$  has been established through theoretical considerations [7,8] and numerical simulations (e.g. [9–12]), and finds support also from

laboratory experiments [13] (see discussion in Ref. [1]).

Statistical mean-field theories have been instrumental for explaining how such coarsening arises from grain-scale kinetics under the space-filling constraints that grains do not overlap and no voids appear as grain boundaries move. These theories describe the process by regarding each grain as embedded in the mean environment of the population [1]. In the Hillert–Mullins-type “drift models” [14,15], the grain-size distribution  $n$  obeys the continuity equation

$$\frac{\partial n}{\partial t} + \frac{\partial}{\partial x}(vn(x, t)) = 0, \quad (2)$$

where the drift velocity  $v (= dx/dt)$  represents grain exchange between different sizes. One would expect that, in a grain system where the rules of grain-boundary migration and associated topological reorganization are all known or prescribed, the evolution can be tracked by a ‘complete’ statistical-mechanical model based on nothing besides the rules, i.e. not involving extraneous assumptions or approximations informed by the actual outcomes of the NGG dynamics. This means that, if Eq. (2) is a valid model, then a self-contained recipe for the velocity  $v$  ought to exist (and hopefully can be found). However, as outlined below, all current models invoke some kind of parameterization for  $v$ : thus there is a knowledge gap.

E-mail address: [f.ng@sheffield.ac.uk](mailto:f.ng@sheffield.ac.uk).

The purpose of this paper is to provide a mean-field model for NGG in 1D that is complete in the above sense. The model takes the form of a partial integro-differential equation (PIDE), not a partial differential equation. We detail its derivation, explore its relationship with Eq. (2) and compare its predictions to direct simulations of the system. As Mullins [15] explained, Eq. (2) stems from a Fokker-Planck formulation and contains no diffusion term (unlike as envisaged in Louat's model [16]) when the growth process is dominated by curvature-driven grain boundary motion rather than stochastic switching events in grain size or network topology. Our work tackles the same regime.

Hillert's [14] original parameterization for the drift velocity is

$$v = \alpha k \left( \frac{1}{x_c} - \frac{1}{x} \right), \quad (3)$$

where  $x_c$  is a time-varying critical grain size ( $\propto \bar{x}$ ),  $k$  is the product of grain-boundary energy and mobility, and  $\alpha$  is an order-one parameter that varies with the number of spatial dimensions in the system. Eq. (3) summarizes the tendency that grains larger than  $x_c$  grow and smaller than  $x_c$  shrink; it assigns a single drift velocity to grains of equal size, even though such grains are neighbored by grains of different sizes so they do not grow or shrink at the same rate. By using techniques of the Lifshitz-Slyozov-Wagner [17,18] theory for coarsening dynamics in solid solutions, Hillert predicted long-time parabolic growth with Eqs. (2) and (3) and calculated the corresponding invariant grain-size distribution. However, since his work, shortcomings of the model has spurred many 'modified' mean-field models seeking to improve the parameterization. A first key shortcoming is that Hillert's invariant grain-size distribution mismatches the invariant distributions found in direct 2D and 3D simulations; e.g. [9–11,19,20]. A second issue, exposed also by simulations, is that "spatial grain size correlations" develop as NGG occurs [21–23], with small grains becoming neighbored by more large grains than expected from  $n(x, t)$  (which is not surprising because the former grains have lost material to the latter), and large grains neighbored by more small grains than expected from  $n(x, t)$  (the former grains have gained material from the latter). This finding conflicts with the idea behind Eq. (3) that different-sized grains evolve under the same environment. Approaches to modify Hillert's drift-velocity parameterization include: (i) pre-multiplying  $1/x_c$  in Eq. (3) by an empirically-tuned function  $f(x/x_c)$  so that the effective critical grain size  $x_{c,eff}$  varies with  $x$  to mimic observed neighbour-size correlations [21,22,24]; and (ii) using topological considerations to formulate alternative functions to link  $v$  to the reduced grain size  $x/\bar{x}$  (e.g. [25–30]). Some of the latter approaches deduce the rate of grain area/volume evolution by accounting for the topological class (number of sides) of the grains (e.g. [30]) and invoke the von Neumann–Mullins 2D growth law [31,32] or its 3D extension [33]. Still other models track the grain-size distributions in different topological classes with separate continuity equations [34,35], although they are not usually considered as being of Hillert-Mullins type. We do not review the large number of modified Hillert theories here but point the reader to the paper by Ref. [36] for further background. Crucially, all modified theories contain adjustable parameters/coefficients that are determined through fitting to the observed dynamics (typically the invariant grain-size distribution). The model derived in this paper has no such necessity.

We see value in investigating a parameterization-free theory. The modified Hillert theories have engendered a tradition of invoking parameterizations to "close" the mean-field description. Such approach is useful because an ansatz posed for the resulting model often yields an analytical solution that can be evaluated straightforwardly for the invariant grain-size distribution. But

parameterizations sacrifice physical understanding of the phenomenon, as the basis of some parameters involved remains incompletely known (their values do not derive from first principles), and both the model and its fit to the observed invariant grain-size distribution are ultimately approximate. The choice of parameterization is also not unique; more parameters could mean higher degrees of freedom for empirical fitting, and different parameterizations can predict parabolic growth with near-identical-looking invariant  $n(x, t)$ . Some modified theories even assume self-similarity for  $n$  as a starting condition. As we shall see, our PIDE model has none of these limitations and captures collaborative grain-growth dynamics to a sophisticated level: it predicts the observed neighbour grain-size correlations, similarity scaling, invariant grain-size distribution, and relationship between  $k$  and the bulk growth rate  $C$  without parameter tuning. The PIDE also tracks system evolution outside the self-similar state. It is not analytically solvable by us so far, but this does not mean it is invalid or inappropriate.<sup>1</sup> We are not suggesting that a 'complete' formulation is superior to the Hillert-based approximate models, but rather it is an essential part of our knowledge of NGG. Note that our model treats NGG in *one dimension* only. However, the insights gained from it suggest there is hope for complete mean-field formulations for NGG in 2D and 3D, despite vastly increased topological complexities. We consider this avenue briefly at the end of the paper.

## 2. Model

### 2.1. One-dimensional NGG system

Fig. 1a shows our system, in which a large population of linear crystals/grains, whose sizes we denote by  $x$  ( $> 0$ ), participates in NGG. Following previous work [37,21,24] we assume (by analogy to curvature-driven kinetics in 2D/3D) that each grain boundary between adjacent grains migrates into the smaller grain at a speed proportional to the difference between their size reciprocals  $1/x$ . Thus a grain of size  $x_0$  having left and right neighbours sized  $x_{1L}$  and  $x_{1R}$  (respectively) grows at the instantaneous rate

$$\dot{x}_0 = k \left[ \left( \frac{1}{x_{1R}} - \frac{1}{x_0} \right) - \left( \frac{1}{x_0} - \frac{1}{x_{1L}} \right) \right], \quad (4)$$

where  $k$  (constant) has the same meaning as in Eq. (3). A grain vanishes when two grain boundaries merge. Although this analogue system is an idealization as there are no curved grain boundaries in 1D, its reduced geometry—grains always having two sides, the only switching events being grain-boundary merging—aims our goal of seeking analytical understanding. (In this regard, even 2D models of NGG lose some of the topological complexity of NGG in 3D.) Moreover, as found by Refs. [21,24] and confirmed by our direct kinetic simulations (Fig. 1b–e), the 1D system displays the essential properties of NGG behaviour: its grain population coarsens following parabolic growth and attains an invariant self-similar  $n(x, t)$  at large time (Fig. 1b–e).

Spatial grain size correlations occur in this 1D system also, as reported by Hunderi and his colleagues [21,24]. These authors put forward a modified Hillert model using Approach (i) described in the Introduction, i.e.

$$v = 2k \left( \frac{f(x/x_c)}{x_c} - \frac{1}{x} \right), \quad (5)$$

<sup>1</sup> Many valid models describing complex phenomena without resorting to parameterizations have not yielded to analytical solution.

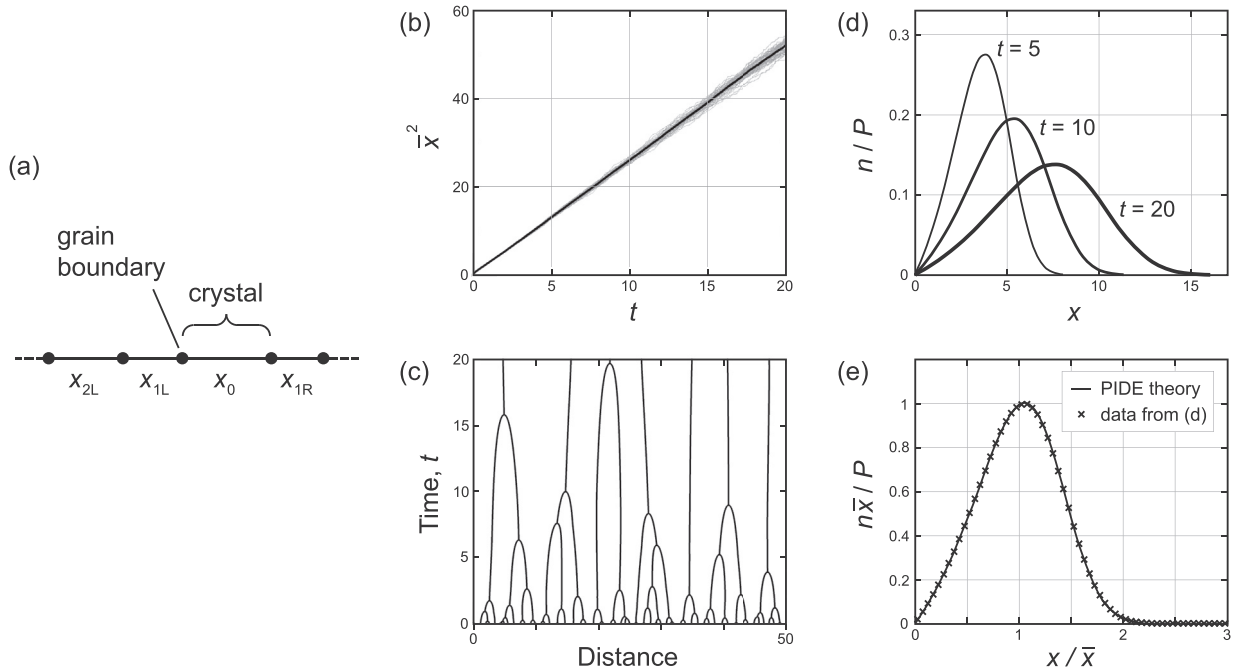


**Fig. 1.** (a) 1D system of interacting grains;  $x$  is crystal/grain size; subscripts label left, far-left, and right neighbours of a crystal of interest (indexed 0). (b)–(e) Results from an ensemble of 20,000 kinetic model simulations with  $k = 1$  unit [ $L^2 T^{-1}$ ]. Each run was initialized with  $10^4$  grains of random size chosen from a uniform probability distribution between  $10^{-5}$  and 1 length unit. (b) Near-linear growth of  $\bar{x}^2$  with time  $t$ ; grey curves plot individual runs; black curve plots their average. (c) Grain-boundary motion and coarsening dynamics in a run. (d) Ensemble mean of normalized grain-size distributions at three times. (e) Invariant grain-size distributions predicted by our mean-field PIDE theory (curve) and from the ensemble runs in (d) (crosses);  $x/\bar{x}$  is reduced grain size.

specifically with

$$f(x/x_c) = \beta_1 + \beta_2 \frac{x}{x_c} + (1 - \beta_1 - \beta_2) \left(\frac{x}{x_c}\right)^2, \tag{6}$$

where  $\beta_1 = 0.702$  and  $\beta_2 = 0.285$  were found by tuning the model to fit simulated correlations. Thus they predicted an analytical invariant grain-size distribution that approximately matches the observed distribution. This model provides additional context for our work below, where we show how the PIDE removes the need for parameterization altogether.

2.2. Statistical-mechanical formulation

Traditional mean-field theories have focussed attention on what happens in the “grain-size space” when deducing the form of the drift velocity  $v$  or the evolution equation for  $n(x, t)$ . But the very occurrence of spatial grain size correlations shows that neighbour interactions lie at the heart of the problem. This clue motivates our radically different formulation here. Rather than address  $n$  directly, we consider how the *size combinations* of neighbouring pairs of grains evolve. We do this by tracking the joint-distribution variable  $g(x, y, t)$ , defined as the number density of grains of size  $x$  having a *left-neighbour* grain of size  $y$ . As this quantification of grain-to-grain relationships applies iteratively to the neighbours of neighbours,  $g$  carries statistical information about the grains’ spatial arrangement, and our formulation automatically captures the long-range impact of each grain’s evolution (via neighbours, to all orders) on the population dynamics. As we shall see, the full grain-growth dynamics are indeed embedded in the “grain size versus neighbour grain size space”—the  $x$ - $y$  plane. This is why tracking grain size alone is not generally sufficient.

Fig. 2 illustrates relevant mathematical concepts. At a given time, each neighbouring pair of grains is located at a point on the  $x$ -

$y$  plane;  $g \, dx \, dy$  counts all pairs within an incremental area. For a system of grains with no directional preference in their ordering (as is assumed here),  $g$  has symmetry:  $g(x,y,t) \equiv g(y,x,t)$ . The physical requirement that there are no infinitely large grains implies  $g \rightarrow 0$  as  $x, y \rightarrow \infty$ . We also expect  $g \rightarrow 0$  as  $x, y \rightarrow 0$  as the system evolves in  $t > 0$ , because, according to Eq. (4), vanishingly small grains—and thus vanishingly small grain neighbours—shrink at rates that ‘blow up’ towards infinity. (Specifically, as one leaves either axis in the perpendicular direction,  $g$  is expected to have a

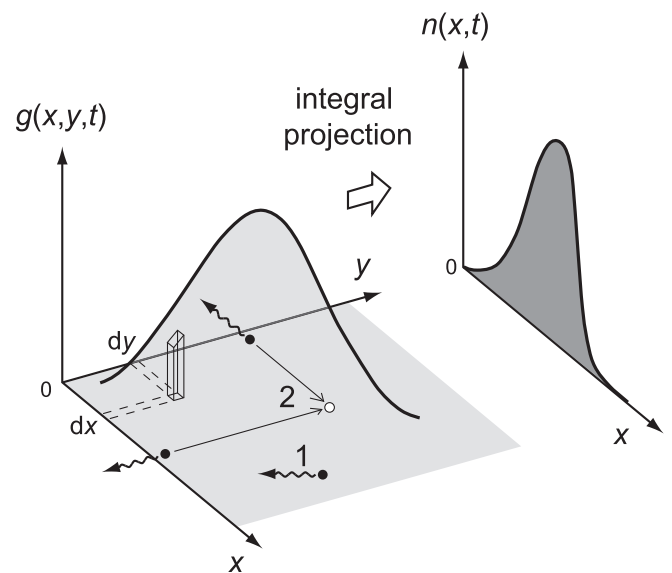


**Fig. 2.** Joint distribution variable  $g(x,y,t)$  and its link to  $n(x,t)$ . Two processes drive the motion of points depicting grain neighbour-pairs: 1. size evolution of a pair without grain elimination; 2. creation of a new pair through grain-boundary merging and elimination of a grain.

positive bounded gradient. This limiting behaviour ensures well-posedness of our PIDE in Eq. (15) below by preventing its terms from becoming singular.) The grain-size distribution is now given by the integral projection

$$n(x, t) = \int_0^{\infty} g(x, y, t) dy. \quad (7)$$

The total length of the domain is time-invariant:

$$L = \int_0^{\infty} xn(x, t) dx, \quad (8)$$

and the population  $P$  and the mean crystal size  $\bar{x}$  are, respectively,

$$P(t) = \int_0^{\infty} n(x, t) dx \quad (9)$$

and

$$\bar{x}(t) = \frac{L}{P}. \quad (10)$$

A key feature of this model is that a population of grains can be ordered differently to exhibit different spatial grain size correlations. This is reflected by the possibility for different joint distributions  $g$  to yield the same  $n(x, t)$  in Eq. (7). The ratio  $g(x, y, t)/n(x, t)$ , which is the probability density distribution of the neighbour size  $y$  for grains sized  $x$ , describes all spatial grain size correlations. Later we show (in Section 4) that this distribution deviates from the normalized grain-size distribution for the population (i.e.  $g(x, y, t)/n(x, t) \neq n(y, t)/P(t)$ ) during statistically self-similar NGG, as is consistent with earlier findings [21–23] that led to queries about the classical mean-field assumption.

Our mean-field evolution equation for  $g$  is now derived. As the system evolves, all points depicting neighbour grain pairs migrate on the  $x$ - $y$  plane (Fig. 2). At any time, pairs of a given size, say  $(x, y) = (x_0, x_{1L})$  (this notation means a grain of size  $x_0$  with a left-neighbour of size  $x_{1L}$ ), are neighbored by grains of different size combinations  $x_{2L}$  and  $x_{1R}$  (see Fig. 1a) so they grow/shrink at different rates. Crucially, the probabilities of these combinations are known from  $g$  instantaneously. The probability of a grain of size  $x$  having on its left (or right) a grain neighbour of size  $y$  to  $y + dy$  is given by

$$p(y|x) = \frac{g(x, y, t)}{n(x, t)} dy. \quad (11)$$

It follows that the fraction of pairs  $(x_0, x_{1L})$  forming the spatial arrangement  $x_{2L}-x_{1L}-x_0-x_{1R}$  is

$$p(x_{1R}|x_0)p(x_{2L}|x_{1L}) = \frac{g(x_0, x_{1R}, t)}{n(x_0, t)} \frac{g(x_{1L}, x_{2L}, t)}{n(x_{1L}, t)} dx_{1R} dx_{2L}. \quad (12)$$

By representing each grain pair as a delta function at  $(x, y) = (x_0, x_{1L})$  moving with velocity  $(\dot{x}_0, \dot{x}_{1L})$  (Process 1 in Fig. 2), where  $\dot{x}_0$  and  $\dot{x}_{1L}$  are known from the kinetic description in Eq. (4), we quantify the effect of the pair's motion on  $g$  by writing:

$$dg = \left( -\dot{x}_0 \frac{\partial}{\partial x} - \dot{x}_{1L} \frac{\partial}{\partial y} \right) \delta(x - x_0, y - x_{1L}) dt. \quad (13)$$

Consequently, the rate of change of  $g$  is found by summing Eq. (13)

over all pairs and all neighbour combinations, using the joint probability in Eq. (12) as weight.

What happens when grain-boundary merging eliminates a grain? This process introduces a source term for  $g$ . Suppose the left-hand grain of a pair is removed:  $x_{1L} \rightarrow 0$ . On the  $x$ - $y$  plane, this event causes the points  $(x_0, x_{1L})$  and  $(x_{1L}, x_{2L})$  representing two pairs to reach the  $x$  and  $y$  axes respectively, and creates an interior point for a new pair  $(x_0, x_{2L})$  (Process 2, Fig. 2). The rate of elimination of the left-neighbours of grains sized  $x_0$  is  $-\lim_{x_{1L} \rightarrow 0} \dot{x}_{1L} g(x_0, x_{1L}, t) dx_0$ , and weighting this by  $p(x_{2L}|x_{1L})$  gives the production rate of new pairs at size  $(x_0, x_{2L})$ .

Taking both of these processes into account now leads to the master equation

$$\begin{aligned} \frac{\partial g}{\partial t} = & \int_0^{\infty} \int_0^{\infty} g(x_0, x_{1L}, t) \int_0^{\infty} \int_0^{\infty} \frac{g(x_0, x_{1R}, t)}{n(x_0, t)} \frac{g(x_{1L}, x_{2L}, t)}{n(x_{1L}, t)} \left( -\dot{x}_0 \frac{\partial}{\partial x} \right. \\ & \left. - \dot{x}_{1L} \frac{\partial}{\partial y} \right) \delta(x - x_0, y - x_{1L}) dx_{1R} dx_{2L} dx_0 dx_{1L} \\ & + \int_0^{\infty} \int_0^{\infty} \lim_{x_{1L} \rightarrow 0} \frac{g(x_{1L}, x_{2L}, t)}{n(x_{1L}, t)} [-\dot{x}_{1L} g(x_0, x_{1L}, t)] \delta(x - x_0, \\ & y - x_{2L}) dx_{2L} dx_0, \end{aligned} \quad (14)$$

where the two right-hand terms describe contributions from grain evolution without and with elimination events, respectively. Substituting for  $\dot{x}_0$  and  $\dot{x}_{1L}$  (using Eq. (4)) and evaluating the limit and integrals yields the first-order partial integro-differential equation (PIDE):

$$\begin{aligned} \frac{\partial g}{\partial t} + k \frac{\partial}{\partial x} \left[ \left( \frac{h(x, t)}{n(x, t)} - \frac{2}{x} + \frac{1}{y} \right) g \right] + k \frac{\partial}{\partial y} \left[ \left( \frac{h(y, t)}{n(y, t)} - \frac{2}{y} + \frac{1}{x} \right) g \right] \\ = 2k \frac{\partial g}{\partial x} \bigg|_{x=0} \frac{\partial g}{\partial y} \bigg|_{y=0} \bigg/ \int_0^{\infty} \frac{\partial g}{\partial x} \bigg|_{x=0} dy. \end{aligned} \quad (15)$$

Here the final source term is due to Process 2,  $n$  has been defined in Eq. (7), and

$$h(x, t) = \int_0^{\infty} \frac{g(x, y, t)}{y} dy. \quad (16)$$

This formulation is complete as it utilized all rules of grain interactions. The PIDE has no tuning parameters because  $k$  is a phenomenological constant.

We acknowledge that alternative rules for the grain-scale kinetics can be supposed for modelling coarsening dynamics in 1D interacting grain systems. Such rule might not involve the reciprocal of the grain size, for instance. A more general form of Eq. (4) is  $\dot{x}_0 = s(x_{1R}, x_0) - s(x_0, x_{1L})$ , where the function  $s(x, y)$  defines the migration speed of the grain boundary between each grain pair. In Appendix I we present the corresponding master PIDE found by the same derivation as the one above.

### 2.3. Preliminary analysis of the PIDE

Eq. (15) with the homogeneous boundary conditions  $g \rightarrow 0$  as  $x, y \rightarrow 0$  and  $\infty$  is to be solved for the non-trivial solution ( $g \neq 0$ ). Although the problem admits any multiples of a solution also as solution, it is nonlinear ( $g_1 + g_2$  is not a solution if  $g_1$  and  $g_2$  are independent solutions) because  $g$  in the advection terms in Eq. (15)

is pre-multiplied by  $h/n$ , a ratio involving  $g$ . Writing this ratio as

$$\frac{h(x, t)}{n(x, t)} = \int_0^\infty \frac{g(x, y, t)}{yn(x, t)} dy = \int_{-\infty}^\infty \frac{g(x, y, t)}{n(x, t)} d(\ln y) \quad (17)$$

shows that it represents a different function for different  $g$ 's yielding the same  $n$ . This means that  $h/n$  encapsulates information about grain spatial ordering.

The pervasiveness of *nonlocal* effects in grain-growth dynamics can be seen from the PIDE structure. Both the advection and source terms in Eq. (15) contain integrals of quantities based on  $g$ , implying that the spatial size-ordering of all grains statistically influences the evolution of every grain pair and the formation rate of new pairs at different sizes (due to grain elimination).

If the spatial arrangement of the grains did not matter to the dynamics, a self-contained description of  $n$  without  $g$  would be possible. We explore this idea by integrating Eq. (15) with respect to  $y$  from 0 to  $\infty$  (see details in Appendix II), which gives

$$\frac{\partial n}{\partial t} + 2k \frac{\partial}{\partial x} \left( h(x, t) - \frac{n}{x} \right) = 0. \quad (18)$$

It is not possible here to get rid of  $h$  (and thus  $g$ ) to obtain a closed problem for  $n$  (as in Continuity Eq. (2)) unless extra constraints come into play to link  $h$  to  $n$ . This result indicates that NGG in 1D cannot be correctly or comprehensively described by the traditional drift model. However, in Section 5 we show that the condition of statistical self-similarity provides a sufficient constraint to close the problem. Thus, tracking of NGG before self-similarity is reached strictly requires the PIDE model, although it can be done with the drift model during self-similar growth.

Eq. (18) also confirms that while the grain-size distribution appears to spread in a diffusion-like manner (Fig. 1d) during NGG, there is, for the 1D system at least, no diffusion term of the kind  $\partial^2 n / \partial x^2$  as posited by Louat [16] in the model.

### 3. Self-similarity

We proceed to study the self-similar properties of the system by using the PIDE model, notably to show that it successfully predicts the observed parabolic growth law.

Model Eqs. (15), (16), (7) and (8) are invariant under the scaling transformations  $t \rightarrow \epsilon t$ ,  $(x, y) \rightarrow \epsilon^{1/2}(x, y)$  and  $g \rightarrow \epsilon^{-3/2}g$ . If we introduce the new time  $\tau = kt$  and let

$$\begin{aligned} G(X, Y, \tau) &= \tau^{3/2}g(x, y, t), & X &= \frac{x}{\tau^{1/2}}, & Y &= \frac{y}{\tau^{1/2}}, \\ N(X, \tau) &= \tau n(x, t), & H(X, \tau) &= \tau^{3/2}h(x, t), \end{aligned} \quad (19)$$

then, in these “similarity variables”, the model becomes

$$\begin{aligned} \frac{\partial G}{\partial(\ln \tau)} - \frac{1}{2} \left( X \frac{\partial G}{\partial X} + Y \frac{\partial G}{\partial Y} + 3G \right) + \frac{\partial}{\partial X} \left[ \left( \frac{H(X, \tau)}{N(X, \tau)} - \frac{2}{X} + \frac{1}{Y} \right) G \right] \\ + \frac{\partial}{\partial Y} \left[ \left( \frac{H(Y, \tau)}{N(Y, \tau)} - \frac{2}{Y} + \frac{1}{X} \right) G \right] &= 2 \frac{\partial G}{\partial X} \Big|_{X=0} \frac{\partial G}{\partial Y} \Big|_{Y=0} \Big/ \int_0^\infty \frac{\partial G}{\partial X} \Big|_{X=0} dY \end{aligned} \quad (20)$$

where

$$N(X, \tau) = \int_0^\infty G(X, Y, \tau) dY \quad \text{and} \quad H(X, \tau) = \int_0^\infty \frac{G(X, Y, \tau)}{Y} dY. \quad (21)$$

The domain length in Eq. (8) remains time-invariant:

$$L = \int_0^\infty XN(X, \tau) dX = \int_0^\infty \int_0^\infty XG(X, Y, \tau) dY dX. \quad (22)$$

Like the original master equation, Eq. (20) is a PIDE. The behaviour of its solution at the boundaries is  $G \rightarrow 0$  as  $X, Y \rightarrow 0$  and  $\infty$ .

The transformation essentially performs a suitable magnification in length-scale to view grain sizes relative to each other as time progresses. NGG becomes statistically self-similar when Eq. (20) reaches its steady state  $\partial/\partial\tau \rightarrow 0$  in the long-time limit; then all dependences on  $\tau$  drop from Eqs. (20)–(22). If we denote the steady-state solution by  $G = G_S(X, Y)$ , then the similarity solution of the untransformed problem is  $g = \tau^{-3/2} G_S(x/\tau^{1/2}, y/\tau^{1/2})$ , and

$$N = N_S(X) = \int_0^\infty G_S(X, Y) dY \quad (23)$$

describes the invariant grain-size distribution in terms of scaled grain size  $X$ ; similarly,  $H$  becomes  $H_S(X)$  in Eq. (21). Because any multiples of  $G_S$  is also a solution, the value of  $L$  specified in the integral constraint in Eq. (22) is arbitrary. For convenience, below we present solutions and simulated forms of  $G_S$  that have been normalized as a probability density distribution (i.e.  $\int_0^\infty \int_0^\infty G_S dY dX = \int_0^\infty N_S dX = 1$ ).

Like  $g(x, y, t)/n(x, t)$  described before,  $G(X, Y, \tau)/N(X, \tau)$  in the transformed problem defines the instantaneous probability density distribution of neighbour size. That this ratio becomes  $G_S(X, Y)/N_S(X)$  (independent of  $\tau$ ) at steady state means that during statistically self-similar NGG, all spatial grain size correlations also become invariant.

Turning to the grain-growth rate, the transformed expression for the grain population in Eq. (9) is

$$P = \tau^{-1/2} \int_0^\infty N_S(X) dX \quad (24)$$

after  $N$  has attained  $N_S(X)$ , so the population decays as  $t^{-1/2}$  at the self-similar state. Correspondingly, the mean grain size ( $= L/P$ ) becomes

$$\bar{x} = \sqrt{kt} \bar{X} \quad (\propto t^{1/2}), \quad (25)$$

in which

$$\bar{X} = \int_0^\infty XN_S dX \Big/ \int_0^\infty N_S dX \quad (26)$$

is the (constant) mean value of  $X$  in the scaled grain-size distribution. We determine  $\bar{X} \approx 1.61$  from the numerical solution of the next section. The PIDE theory thus predicts  $m = 1/2$  in Eq. (1) with

$$C = k\bar{X}^2 \approx 2.6k, \quad (27)$$

which agrees with the mean coarsening rate observed in the ensemble simulations in Fig. 1b (where  $k = 1$ ). Note that the parabolic growth law predicted here is a universal result for one-dimensional NGG that holds for any  $k$ , and it derives from the kinetic description of the system without any assumed parameterizations or fitting.

#### 4. Numerical solution

In modified Hillert theories, a common practice is to fit the predicted invariant grain-size distribution to the simulated distribution by tuning parameters in the drift velocity. In our PIDE theory, no tuning is possible. The question is simply whether it predicts the observed grain-size distribution and correlations.

Analytical solution of the steady-state form of the PIDE (20)

$$-\frac{1}{2} \left( X \frac{\partial G_S}{\partial X} + Y \frac{\partial G_S}{\partial Y} + 3G_S \right) + \frac{\partial}{\partial X} \left[ \left( \frac{H_S(X)}{N_S(X)} - \frac{2}{X} + \frac{1}{Y} \right) G_S \right] + \frac{\partial}{\partial Y} \left[ \left( \frac{H_S(Y)}{N_S(Y)} - \frac{2}{Y} + \frac{1}{X} \right) G_S \right] = 2 \frac{\partial G_S}{\partial X} \bigg|_{X=0} - \frac{\partial G_S}{\partial Y} \bigg|_{Y=0} + \int_0^\infty \frac{\partial G_S}{\partial X} \bigg|_{X=0} dY \quad (28)$$

or its original untransformed version (Eq. (15)) can yield valuable insights into NGG dynamics, but doing this presents obstacles. As noted before, the PIDE has nonlocal advection terms and is nonlinear. The nonlinearity rules out series expansion and integral transform methods. Although nonlocal advection equations arise in other continuum-mechanical contexts (e.g. [38]), analytical techniques for solving them are not well developed. Logan [39] used the method of characteristics to solve a first-order nonlocal advection equation, but the occurrence in our PIDE of both a source term and the ratio of integrals  $H_S/N_S$  (or  $h/n$ ) in the advection terms makes the trajectories of characteristics difficult to anticipate before the solution has been found. Exploiting the  $x$ - $y$  symmetry of the problem has also not led us to progress. However, it suffices for our goal in this paper to demonstrate the model's success by solving it numerically. We therefore leave the analytical solution (of Eq. (28), or (20) or (15)) as an open problem for the community to tackle. We reiterate that a model's validity rests on the rigour of its

formulation and how well it explains the phenomenon, not on its analytical solubility. That the PIDE is non-trivial to solve reflects the true complexity of 1D NGG.

Here we show numerically that the steady-state solution  $G_S(X,Y)$  correctly predicts the long-time invariant grain-size statistics of the system found from direct kinetic simulations. To compute  $G_S$ , we use a finite-difference scheme to evolve  $G$  in Eq. (20) forward in time ( $\ln \tau$ ) until steady state, starting with an initial distribution representing small grains,  $G \propto XY \exp[-(X^2+Y^2)]$ . Some quantities (notably  $H/N$ ) are evaluated at staggered grid points in the scheme. This approach is equivalent to relaxational methods that introduce a fictitious time derivative in Eq. (28) to let  $G_S$  converge.

Fig. 3 compares the numerical results of our PIDE theory to ensemble-mean results from  $10^6$  direct simulations. As in the simulations reported in Fig. 1, each run here started with  $10^4$  grains of random length chosen from a uniform probability distribution between  $10^{-5}$  and 1 units.  $G_S(X,Y)$  is found to be symmetrical about  $X = Y$  (as expected) and single-humped (Fig. 3a), and matches the normalized form of  $g(x,y,t)$  compiled from the ensemble runs (Fig. 3b) at  $t = 40$ , a time far into the self-similarity regime (Fig. 1b and d). This match implies that spatial grain size correlations are automatically reproduced by the theory, as shown in Fig. 3d, which compares the neighbour-size probability density distribution  $G_S(X,Y)/N_S(X)$  at four values of reduced grain size against results from the ensemble runs. The way these distributions deviate from the grain-size distribution of the population (black curve, Fig. 3d) confirms the spatial grain size correlations found in earlier studies [21,24]. As the deviations show that transsects of  $G_S(X,Y)$  at different values of  $X$  or  $Y$  are dissimilar in shape (this is also apparent from the planform of  $G_S$  in Fig. 3a), we know that  $G_S$  is not separable as the product of a function of  $X$  and a function of  $Y$ , and consequently the PIDE cannot be solved analytically by such separation. [Notice that if  $G_S$  were separable as  $G_S = f(X)f(Y)$  symmetrically, normalization of  $G_S$  as a probability density distribution would imply

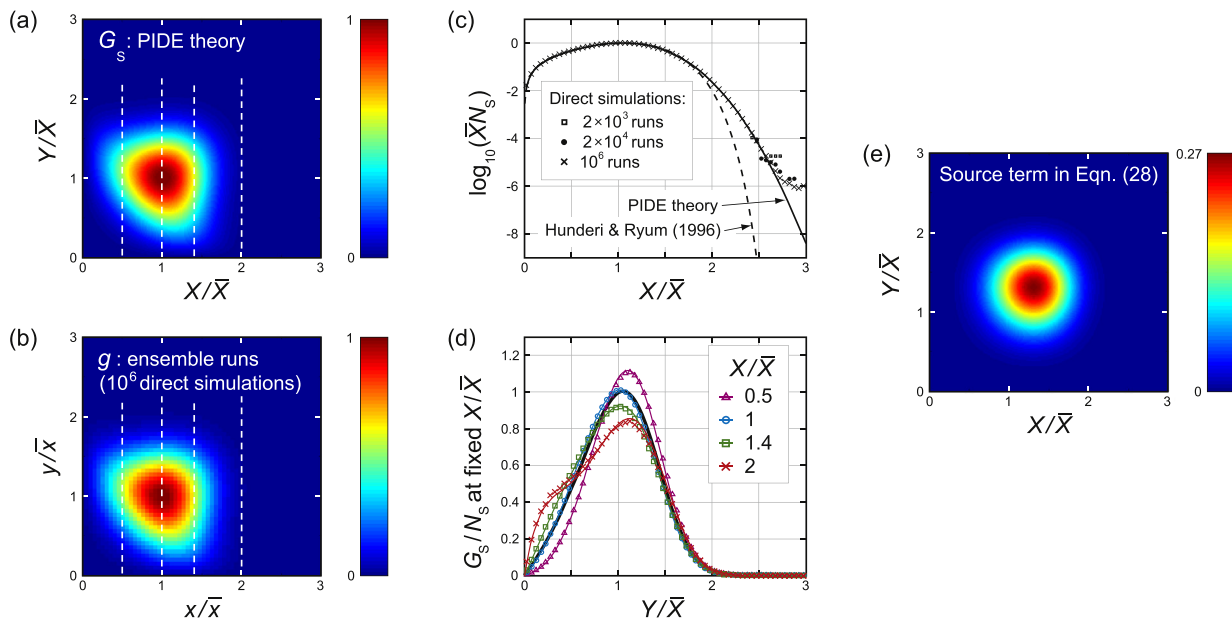


**Fig. 3.** Predictions of mean-field (PIDE) theory tested against results from direct kinetic simulations. Reduced grain sizes are used to ensure comparability. (a) Steady-state solution  $G_S$  of Eq. (20), normalized to form a probability density function over grain size vs. neighbour-grain size space. (b) Ensemble mean of  $g(x,y,t)$  at  $t = 40$  from  $10^6$  simulations of the kind used in Fig. 1b–e. (c) Normalized invariant grain-size distribution  $N_S$  from Eq. (23) (solid curve), plotted in logarithmic frequency axis and compared to simulated data (crosses) and to the modified Hillert theory of Hunderi and Ryum [21] (dashed). Squares and dots plot simulated data in the distribution's tail from smaller ensembles. (d) Neighbour-size probability density distributions  $G_S(X,Y)/N_S(X)$  (curves) at four values of  $X/\bar{X}$  compared with simulated data (symbols, coloured the same as the curves). These transsects are located by white lines in (a) and (b). Black curve plots the normalized form of  $N_S$ . (e) Rate of new grain-pair production (source term on the right-hand side of Eqs. (20) and (28)) as a function of  $X/\bar{X}$  and  $Y/\bar{Y}$ .

$\int_0^\infty f(X) dX = 1$ . Then  $f(X) \equiv N_S(X)$  follows from Eq. (23) and the neighbour-size probability density distribution would be given by  $G_S(X,Y)/N_S(X) \equiv N_S(Y)$ . In other words, the erroneous assumption that grain neighbours have a size distribution identical to the population's grain-size distribution would be true.]

Fig. 1e shows the agreement between the invariant grain-size distribution  $N_S(X)$  predicted by the PIDE (which we compute from  $G_S$  using Eq. (23)) and the ensemble-mean invariant grain-size distribution found from the direct simulations. It is typical for modified Hillert theories [21,22,24–29] and function-based approximations (e.g. [40]) of grain-size distributions during self-similar NGG to evaluate this kind of match in linear scale, as done in Fig. 1e. Few studies examine discrepancies in the tail of the distribution in order to discern deficient model behaviour at large grain sizes. To see how well our theory captures the tail, in Fig. 3c we replot the comparison of Fig. 1e in logarithmic scale. The agreement between theory and data at  $X/\bar{X} (= x/\bar{x}) < 2$  visible in linear scale is again found. Mismatch becomes noticeable at  $X/\bar{X} > 2.5$  but this occurs at low probability density ( $N_S < 10^{-4}$ ) with small absolute errors ( $< 10^{-5}$ ). Crucially, as we increase the number of ensemble runs used to calculate the invariant distribution towards  $10^6$ , more and more of the simulated data points at large grain size reach the theoretical curve (see different symbols in Fig. 3c) and the errors decrease (to  $< 10^{-6}$ ). This convergence and the alignment of the curve with the points show that the PIDE theory captures the tail of the distribution with remarkable precision.

Numerically, an imperfect match at arbitrarily large  $X/\bar{X}$  between theory and ensemble simulation is always expected due to rounding errors and discretization of time in the kinetic simulations, and because the simulations produce few large grains whose statistics must be found by averaging over many runs. Furthermore, since the simulated grain size is finite, grain counts must become zero at a sufficiently large size. Given the simulations have a fixed domain length, the resulting deficit in probability density causes a slight overestimation of probability density at all sizes registering non-zero grain counts. This explains why the simulated data points in the tail in Fig. 3c tend to approach the curve of the PIDE theory from above.

For comparison, in Fig. 3c we include the grain-size distribution predicted for the same 1D NGG system by the modified Hillert model of Hunderi and Ryum [21], which assumes the drift-velocity parameterization in Eqs. (5) and (6). Their model predicts an overstep decay that underestimates the abundance of grains at  $X/\bar{X} > 2$ .

A final discovery from our numerical solution, revealed by the distribution of the source term of Eq. (28) plotted in Fig. 3e, is that most new neighbour pairs produced through the elimination of small grains contain grains that are larger than the most frequent or modal grain size (which turns out to be  $\approx \bar{X}$ ). This result makes sense because these larger grains eliminate their small neighbours faster despite their lower abundance.

### 5. Validating and informing the Hillert-type drift model with the PIDE theory

In this section, we extend our analysis of the PIDE to explain why the traditional drift model validly describes 1D NGG during statistical self-similarity—and only in this state. We also calculate an explicit expression for the corresponding drift velocity.

Recall that our effort in Section 2.3 to derive an evolution equation for  $n$  from the PIDE had led to Eq. (18), here rewritten slightly as:

$$\frac{\partial n}{\partial t} + \frac{\partial}{\partial x} \left[ 2k \left( \frac{h}{n} - \frac{1}{x} \right) n \right] = 0. \tag{29}$$

Comparing this to the general continuity equation (2) identifies the

drift velocity to be

$$v = 2k \left( \frac{h(x,t)}{n(x,t)} - \frac{1}{x} \right). \tag{30}$$

Although this drift velocity does not close the problem for  $n$  (Section 2.3), it resembles and supports the mathematical form of the parameterizations assumed in the Hillert-type models, which posit  $v$  as being proportional to  $1/x_c - 1/x$ , where  $x_c$  is the critical grain size (Section 1).

Eq. (30) specifically implies that the instantaneous reciprocal value of  $x_c$  is given by

$$x_c^{-1} = \frac{h(x,t)}{n(x,t)} = \tau^{-1/2} \frac{H(X,\tau)}{N(X,\tau)}, \tag{31}$$

where  $h/n$  carries information about grain spatial ordering (Section 2.3). Hitherto in this analysis, it is not in fact known whether  $h/n$  has the right dependence on  $x$  to make  $x_c$  behave such that large grains grow and small grains shrink—we confirm this to be the case below. However, the final transformation in Eq. (31), which casts  $x_c$  in the similarity variables, shows that during statistically self-similar NGG we have  $x_c \propto \tau^{1/2}$  (since  $N \equiv N_S(X)$  and  $H \equiv H_S(X)$ ), just as  $x$  does, as indicated by the scaling in Eq. (19). What this means is that during self-similar growth, there is a unique recipe for  $x_c$  dependent on the reduced grain size—but independent of  $\tau$ —that closes the drift model. The reason for this is that all scaled spatial grain size correlations are then invariant (this is the constraint mentioned in Section 2.3). Away from the similarity state, no such recipe exists because spatial grain size correlations are varying: then the drift model must break down.

Next we establish this outcome formally, determining the ratio  $H_S(X)/N_S(X)$  (and thus  $x_c^{-1}$ ) at the same time. First, transforming Eq. (29) with Eq. (19) yields:

$$\frac{\partial N}{\partial(\ln \tau)} - \frac{1}{2} \left( X \frac{\partial N}{\partial X} + 2N \right) + 2 \frac{\partial}{\partial X} \left( H(X) - \frac{N}{X} \right) = 0. \tag{32}$$

Under the self-similarity condition,  $\partial/\partial(\ln \tau) = 0$ ,  $N = N_S(X)$  and  $H = H_S(X)$  so that

$$-\frac{1}{2} \left( X \frac{dN_S}{dX} + 2N_S \right) + 2 \frac{d}{dX} \left( H_S(X) - \frac{N_S}{X} \right) = 0. \tag{33}$$

(Another way to find this result is to integrate Eq. (28) w.r.t.  $Y$  from 0 to  $\infty$ .) Eq. (33) can be integrated once, with the knowledge (from (21)) that  $H_S = 0$  as  $X \rightarrow \infty$ , to give

$$H_S(X) = \left( \frac{X}{4} + \frac{1}{X} \right) N_S - \frac{1}{4} \int_X^\infty N_S(X) dX. \tag{34}$$

As  $H_S$  vanishes also at  $X = 0$ , it follows that

$$\lim_{X \rightarrow 0} \frac{N_S(X)}{X} = \frac{\partial N_S}{\partial X} \Big|_{X=0} = \frac{1}{4} \int_0^\infty N_S(X) dX = \frac{1}{4} \tag{35}$$

(if we assume  $N_S$  has been normalized). The slope predicted here for  $N_S$  at the origin is confirmed by our numerical solution. The preceding series of steps parallel the mathematical derivation of Hunderi and Ryum's [41] well-known result that the invariant grain-size distribution and reduced grain-growth rate are uniquely related at the similarity state. The difference here is that the PIDE tells us the exact form of the drift velocity. Also, the step between Eqs. (32) and (33) shows that the ratio  $H/N$  cannot be invariant of  $\tau$

away from self-similarity.

Armed with Eq. (34), we now write the reciprocal of the critical grain size during statistically self-similar NGG as  $x_c^{-1} = \tau^{-1/2} H_S(X)/N_S(X)$ , where

$$\frac{H_S(X)}{N_S(X)} = \frac{X}{4} + \frac{1}{X} - \frac{1}{4N_S} \int_X^\infty N_S(X) dX. \quad (36)$$

In terms of untransformed variables, the corresponding drift velocity is

$$v = \frac{1}{2t} \left( x - \frac{1}{n} \int_x^\infty n(x, t) dx \right). \quad (37)$$

Note that substituting Eq. (37) back into the continuity equation (29) leads to  $t(\partial n/\partial t) + (x/2)(\partial n/\partial x) = -n$ , which merely ascertains the similarity scaling in Eq. (19). Determining the form of  $n(x, t)$  or  $N_S(X)$  still requires solving the PIDE for  $g$  or  $G_S$ .

From the foregoing analysis, it should be clear that the parameterized form  $f(x/x_c)/x_c$  in the modified Hillert theory of Hunderi and Ryum [21] (Eq. (5) and (6) in Section 2.1) serves to approximate  $h/n$ . It is interesting to compare their parameterization to the exact drift velocity known from our theory. This can be done by writing  $v$  in terms of the reduced grain size  $\rho = x/\bar{x} = X/\bar{X}$ , i.e.

$$v = \frac{2k}{\bar{x}} \left( \frac{1}{\rho_c} - \frac{1}{\rho} \right), \quad (38)$$

where  $\rho_c$ , the reduced effective critical grain size, is given by

$$\frac{1}{\rho_c} = \begin{cases} \bar{X} \frac{H_S(\bar{X}\rho)}{N_S(\bar{X}\rho)} & \text{(PIDE theory)} \\ c_0 f(c_0\rho) & \text{(Hunderi & Ryum)} \end{cases}. \quad (39)$$

The constant  $c_0 (= 1.229)$  is the ratio of  $\bar{x}$  to  $x_c$  in Hunderi and Ryum's theory [21].

Fig. 4 plots the two functions on the right-hand side of Eq. (39) against  $\rho$ . (Our evaluation of  $H_S/N_S$  uses Eq. (36) and the numerically-computed form of  $N_S(X)$  from Section 4.) Comparing the functions with  $1/\rho$  (dashed-dotted line) shows that they both predict growth for large grains and shrinkage for small grains. Hunderi and Ryum denoted their function “ $G_1(\rho)$ ” and called it the “quasi-stationary correlation function” (see Ref. [21] and their Fig. 4a). It deviates from our result and overestimates the drift velocity near  $\rho = 0$  and at  $\rho \geq 1.5$ . Notably, as  $\rho \rightarrow \infty$ , our function asymptotes towards a constant slope ( $\bar{X}^2/4$ ) whereas their parabolic function continues to steepen (see Eq. (6)); we suspect this to be responsible for the inaccurate tail of their invariant grain-size distribution (Fig. 3c). Their function also misses out the sharp change in  $1/\rho_c$  for small  $\rho$ ; this illustrates how much an assumed parameterization can misrepresent the actual dynamics.

## 6. Discussions and conclusion

We have formulated an exact and complete statistical mean-field model of NGG in one dimension. Taking the form of a partial integro-differential equation (PIDE), the model accounts for all kinetic interactions of the system and matches key aspects of the observed dynamics (including spatial grain size correlations) without tuning. In fact it lacks tunable parameters: the constant  $k$  describing grain-boundary migration rate is prescribed, as in the direct simulations used to test the model. In contrast, the modified

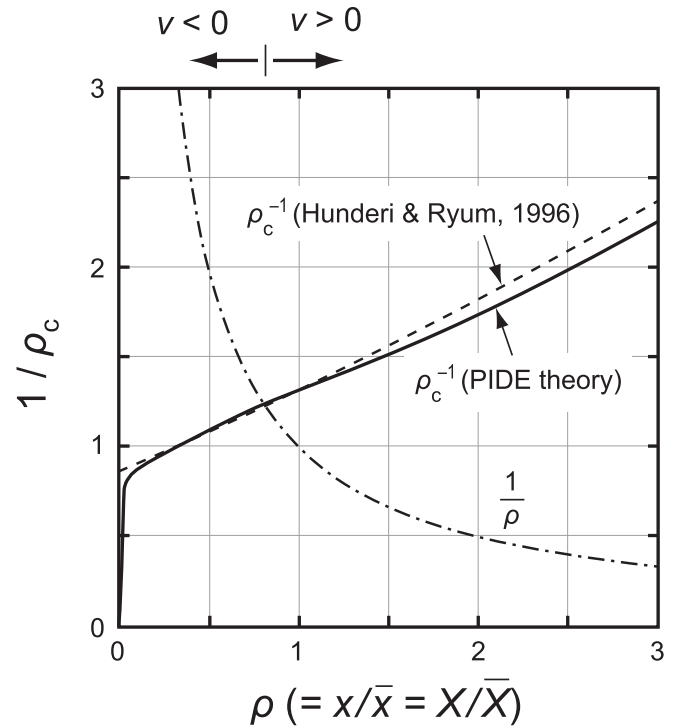


Fig. 4. Dependences, against reduced grain size  $\rho$ , of the reciprocal of the effective reduced critical grain size  $1/\rho_c$  predicted by our PIDE theory (solid) and the same quantity predicted by the modified Hillert theory of Hunderi and Ryum [21] (dashed curve).

Hillert model developed by Ref. [21] for the same NGG system necessitates a drift-velocity parameterization to close the description. In our view, models that parameterize physics and require tuning afterwards essentially make an engineering approximation to predict nearly the right result.

Whereas the Hillert-type drift models are valid only in the self-similar state of NGG (only then does a well-defined drift velocity exist), the PIDE captures the statistical mechanics generally (including outside that state), because its formulation does not rely on assumptions of self-similarity or scaling. Whether one considers the PIDE model or modified Hillert models to be more useful depends on the scientific context. We imagine that for physicists wanting to understand NGG from first principles, the PIDE theory provides a more fundamental and rigorous starting point.

As far as we know, the PIDE in Eqs. (7), (15) and (16) (or its transformed version in Eqs. (20) and (21)) has not been described before. We solved it numerically in this study; its analytical solution remains outstanding. Future work should investigate the stability of the transformed PIDE to determine under what conditions  $G_S$  behaves as an attractor of  $G$ . Such study may yield insights into abnormal grain growth, in which a few large grains grow much faster than the rest of the population to cause a non-scale-invariant, bimodal grain-size distribution [14,42]. Following the theoretical framework of [43], we regard the similarity solution of our PIDE not only as a special-case solution, but also as the “intermediate asymptotics” of the system's evolution when it is far from equilibrium but when it no longer depends on the details of the initial conditions (i.e. when mean grain size  $\bar{x}$  far exceeds its initial value). Naturally, when  $\bar{x}$  grows to nearly the size of the polycrystal, edge effects can destroy the self-similarity and there may be too few grains for the mean-field description to be appropriate.

The role of nonlocal effects—stemming from neighbour-to-neighbour interactions between grains—in the collaborative grain

dynamics is recognized throughout our study. These effects, which cause the observed spatial grain size correlations, motivate our use of the joint distribution function  $g(x, y, t)$  in the model formulation and explain why integrals of  $g$  appear in the master equation to render it a PIDE.

Nothing suggests to us that similar nonlocal effects are absent from higher-dimensional NGG, especially as there is evidence of spatial correlations in grain size and in grain-boundary network topology from simulations [22,23,44]. Consequently, using a joint distribution function may enable the development of complete statistical mean-field models of NGG in 2D and 3D also. Although pursuing these descriptions is beyond the scope of this paper, some of the key ingredients and obstacles can be anticipated. In 2D (/3D), most grains will have more than 3 (/4) neighbours so grain “pairing” occurs in many directions, and each grain’s geometry demands more characterization than size alone. The kinetic description must also specify the rules of topological reorganizations of the grain-boundary network, namely those causing neighbour switching events and changes in the topological classes (number of sides) of grains [34,35,44]. Potentially, a joint distribution function akin to  $g$  can be used to quantify the frequency of different combinations of geometrical variables across multiple adjacent grains. It will involve a large number of independent variables (cf.  $x$  and  $y$  in our model). Despite the level of mathematical complexity involved, as before we expect the grain-size distribution to be given by an integral projection, and the master equation to emerge as a PIDE (or system of PIDEs). Based on what we have learned from the 1D system, it is likely that a complete mean-field theory of this kind will also enrich the foundation behind the range of existing parameterized models of 2D/3D NGG dynamics. Research that complements this line of enquiry is already under way. Barmak et al. [45,46] recently explored a new statistical approach to model critical events in the reconfiguration of the grain-boundary network during NGG. Interestingly, their description also involves PIDEs.

More generally, we suggest that the emergence of correlated spatial structures may be an inherent property of many other evolving networks and cellular systems (besides NGG) where neighbour interactions conspire to give the agglomerated behaviour. Nonlocal PIDEs may be essential for understanding these systems.

**Acknowledgements**

I thank an anonymous reviewer for valuable suggestions on the manuscript, and A. Fowler, M. McGuinness, I. Moyles, E. Benilov, J. Gleeson, S. Mitchell and S. O’Brien for stimulating discussions when I presented this work during a visit to their mathematical research group (MACSI) in the University of Limerick in December 2015.

**Appendix I: Generalized PIDE for  $g$**

Let  $s$  be the migration speed of the grain boundary between each grain pair  $(x, y)$ , taken positive if the boundary moves to the right;  $y$  is the size of the left-hand grain as before. For consistent kinetics regardless of how direction is defined, the function  $s(x, y)$  must be antisymmetric:  $s(x, y) = -s(y, x)$ ; thus,  $s(x, x) = 0$  for all  $x$ . Grain-boundary migration towards the smaller grain requires  $s > 0$  when  $y > x$ . We expect this condition to cause coarsening dynamics because all grains smaller than their two neighbours will shrink (and be eliminated if they remain to be so), although different functional forms for  $s$  are still possible. For example, whereas we assumed  $s(x, y) = k(1/x - 1/y)$  in our analysis in the paper, Ref. [47] investigated coarsening in a system where  $s(x, y) = k(y - x)$ .

Eq. (4) is replaced by the general kinetic description:

$$\dot{x}_0 = s(x_{1R}, x_0) - s(x_0, x_{1L}). \tag{A.1}$$

The evaluation of Eq. (14), with  $\dot{x}_0$  and  $\dot{x}_{1L}$  now given by Eq. (A.1), yields the PIDE

$$\begin{aligned} \frac{\partial g}{\partial t} + \frac{\partial}{\partial x} \left[ \left( s(y, x) - \frac{J(x, t)}{n(x, t)} \right) g \right] + \frac{\partial}{\partial y} \left[ \left( s(x, y) - \frac{J(y, t)}{n(y, t)} \right) g \right] \\ = \frac{\frac{\partial g}{\partial x} \Big|_{x=0} \lim_{\xi \rightarrow 0} [ -g(x, \xi, t)(s(x, \xi) - s(\xi, x)) ]}{\int_0^\infty \frac{\partial g}{\partial x} \Big|_{x=0} dy}, \end{aligned} \tag{A.2}$$

where we have used the definition

$$J(x, t) = \int_0^\infty s(x, y)g(x, y, t) dy. \tag{A.3}$$

(With our assumed function for  $s(x, y)$ , this integral is given by  $J = k [n(x, t)/x - h(x, t)]$ .) The far-field boundary conditions  $g \rightarrow 0$  as  $x, y \rightarrow \infty$  remain valid. However, the behaviour of  $g$  as  $x, y \rightarrow 0$ , as well as the value of the limit in Eq. (A.2), will depend on the functional form of  $s(x, y)$  at those limits.

**Appendix II**

Integrating Eq. (15) with respect to  $y$  from 0 to  $\infty$  leads to

$$\begin{aligned} \frac{\partial}{\partial t} \int_0^\infty g dy + k \frac{\partial}{\partial x} \left[ \left( \frac{h(x, t)}{n(x, t)} - \frac{2}{x} \right) \int_0^\infty g dy + \int_0^\infty \frac{g}{y} dy \right] \\ + k \left[ \left( \frac{h(y, t)}{n(y, t)} - \frac{2}{y} + \frac{1}{x} \right) g \right]_{y=0}^{y=\infty} \\ = 2k \frac{\partial g}{\partial y} \Big|_{y=0} \end{aligned}$$

or, after using the definitions for  $n$  and  $h$  in Eqs. (7) and (16),

$$\begin{aligned} \frac{\partial n}{\partial t} + 2k \frac{\partial}{\partial x} \left( h(x, t) - \frac{n(x, t)}{x} \right) + k \left[ \frac{h(y, t)}{n(y, t)} g \right]_{y=0}^{y=\infty} + \frac{k}{x} g \Big|_{y=0}^{y=\infty} \\ - 2k \frac{g}{y} \Big|_{y=0}^{y=\infty} \\ = 2k \frac{\partial g}{\partial y} \Big|_{y=0}. \end{aligned} \tag{A.4}$$

Now, the boundary behaviour  $g \rightarrow 0$  at  $y = 0$  and as  $y \rightarrow \infty$  implies that  $g \Big|_{y=0}^{y=\infty} = 0$  and

$$\frac{g}{y} \Big|_{y=0}^{y=\infty} = 0 - \lim_{y \rightarrow 0} \frac{g}{y} = - \frac{\partial g}{\partial y} \Big|_{y=0}.$$

If we anticipate that  $h(y, t)g(x, y, t)/n(y, t)$  vanishes when  $y = 0$  and  $y \rightarrow \infty$ , as verified by our numerical solution, then the result in Eq. (A.4) reduces to

$$\frac{\partial n}{\partial t} + 2k \frac{\partial}{\partial x} \left( h(x, t) - \frac{n}{x} \right) = 0. \tag{A.5}$$

## References

- [1] H.V. Atkinson, Theories of normal grain growth in pure single phase systems, *Acta Metall.* 36 (1988) 469–491.
- [2] J.P. Platt, W.M. Behr, Grain size evolution in ductile shear zones: implications for strain localization and the strength of the lithosphere, *J. Struct. Geol.* 33 (2011) 537–550.
- [3] W.W. Mullins, The statistical self-similarity hypothesis in grain growth and particle coarsening, *J. Appl. Phys.* 59 (4) (1986) 1341–1349.
- [4] J. Lambert, R. Mokso, I. Cantat, P. Cloetens, J.A. Glazier, F. Graner, R. Delannay, Coarsening foams robustly reach a self-similar growth regime, *Phys. Rev. Lett.* 104 (2010) 248304.
- [5] M. Castro, R. Cuerno, M.M. García-Hernández, L. Vázquez, Pattern-wavelength coarsening from topological dynamics in silicon nanofoams, *Phys. Rev. Lett.* 112 (2014) 094103.
- [6] C. Castellano, S. Fortunato, V. Loreto, Statistical physics of social dynamics, *Rev. Mod. Phys.* 81 (2009) 591–646.
- [7] J. Burke, D. Turnbull, Recrystallization and grain growth, *Prog. Metal. Phys.* 3 (1952) 220–292.
- [8] W.W. Mullins, J. Viñals, Self-similarity and growth kinetics driven by surface free energy reduction, *Acta Metall.* 37 (1989) 991–997.
- [9] M.P. Anderson, D.J. Srolovitz, G.S. Grest, P.S. Sahni, Computer simulation of grain growth—I. kinetics, *Acta Metall.* 32 (1984) 783–791.
- [10] F. Wakai, N. Enomoto, H. Ogawa, Three-dimensional microstructural evolution in ideal grain growth—general statistics, *Acta Mater* 48 (2000) 1297–1311.
- [11] C.E. Krill III, L.-Q. Chen, Computer simulation of 3-D grain growth using a phase-field model, *Acta Mater* 50 (2002) 3057–3073.
- [12] M. Elsey, S. Eshedoglu, P. Smereka, Large-scale simulation of normal grain growth via diffusion-generated motion, *Proc. Roy. Soc. A467* (2011) 381–401.
- [13] J.A. Glazier, S.P. Gross, J. Stavans, Dynamics of two-dimensional soap froths, *Phys. Rev. A* 36 (1987) 306–310.
- [14] M. Hillert, On the theory of normal and abnormal grain growth, *Acta Metall.* 13 (1965) 227–238.
- [15] W.W. Mullins, Grain growth of uniform boundaries with scaling, *Acta Mater.* 46 (1998) 6219–6226.
- [16] N.P. Louat, On the theory of normal grain growth, *Acta Metall.* 22 (1974) 721–724.
- [17] I.M. Lifshitz, V.V. Slyozov, The kinetics of precipitation from supersaturated solid solutions, *J. Phys. Chem. Solids* 19 (1961) 35–50.
- [18] C. Wagner, Theorie der Alterung von Niederschlägen durch Umlösen (Ostwald-Reifung), *Z. Electrochem* 65 (1957) 581–591.
- [19] D.J. Srolovitz, M.P. Anderson, P.S. Sahni, G.S. Grest, Computer simulation of grain growth—II. grain size distribution, topology, and local dynamics, *Acta Metall.* 32 (1984) 793–802.
- [20] P.R. Rios, T.G. Dalpian, V.S. Brandão, J.A. Castro, A.C.L. Oliveira, Comparison of analytical grain size distributions with three-dimensional computer simulations and experimental data, *Scr. Mater.* 54 (2006) 1633–1637.
- [21] O. Hunderi, N. Ryum, The influence of spatial grain size correlation on normal grain growth in one dimension, *Acta Mater* 44 (1996) 1673–1680.
- [22] K. Marthinsen, O. Hunderi, N. Ryum, The influence of spatial grain size correlation and topology on normal grain growth in two dimensions, *Acta Mater.* 44 (1996) 1681–1689.
- [23] M.W. Nordbakke, N. Ryum, O. Hunderi, Invariant distributions and stationary correlation functions of simulated grain growth process, *Acta Mater.* 50 (2002) 3661–3670.
- [24] O. Hunderi, J. Friis, K. Marthinsen, N. Ryum, Grain size correlation during normal grain growth in one dimension, *Scr. Mater* 55 (2006) 939–942.
- [25] T.O. Saetre, O. Hunderi, N. Ryum, Modelling grain growth in two dimensions, *Acta Metall.* 37 (1989) 1381–1387.
- [26] S.P.A. Gill, A.C.F. Cocks, An investigation of mean-field theories for normal grain growth, *Phil. Mag. A75* (1997) 301–313.
- [27] P.R. Rios, K. Lücke, Comparison of statistical analytical theories of grain growth, *Scr. Mater* 44 (2001) 2471–2475.
- [28] D. Zöllner, P. Streitenberger, Three-dimensional normal grain growth: Monte Carlo Potts model simulation and analytical mean field theory, *Scr. Mater* 54 (2006) 1697–1702.
- [29] P. Streitenberger, D. Zöllner, Effective growth law from three-dimensional grain growth simulations and new analytical grain size distribution, *Scr. Mater* 55 (2006) 461–464.
- [30] P. Streitenberger, D. Zöllner, Triple junction controlled grain growth in two-dimensional polycrystals and thin films: self-similar growth laws and grain size distributions, *Acta Mater* 78 (2014) 114–124.
- [31] J. von Neumann, Written discussion of grain shapes and other metallurgical applications of topology, in: *Metal Interfaces, 1952*, pp. 108–110. Am. Soc. Metals, Cleveland.
- [32] W.W. Mullins, Two-dimensional motion of idealized grain boundaries, *J. Appl. Phys.* 27 (8) (1956) 900–904.
- [33] R.D. MacPherson, D.J. Srolovitz, The von Neumann relation generalized to coarsening of three-dimensional microstructures, *Nature* 446 (2007) 1053–1055.
- [34] V.E. Fradkov, A theoretical investigation of two-dimensional grain growth in the 'gas' approximation, *Phil. Mag. Lett.* 58 (1988) 271–275.
- [35] V.E. Fradkov, D. Udler, Two-dimensional normal grain growth: topological aspects, *Adv. Phys.* 43 (1994) 739–789.
- [36] J. Jeppsson, J. Ågren, M. Hillert, Modified mean field models of normal grain growth, *Acta Mater* 56 (2008) 5188–5201.
- [37] M.A. Fortes, V. Ramos, A. Soares, Grain growth in one dimension: the mean field approach, *Mat. Sci. Forum* 94–96 (1992) 337–344.
- [38] Q. Du, J.R. Kamm, R.B. Lehoucq, M.L. Parks, A new approach for a nonlocal, nonlinear conservation law, *SIAM J. Appl. Math.* 72 (2012) 464–487.
- [39] J.D. Logan, Nonlocal advection equations, *Int. J. Sci. Math. Educ.* 34 (2003) 271–277.
- [40] D. Zöllner, P. Streitenberger, Grain size distributions in normal grain growth, *Prakt. Metallogr.* 47 (2010) 262–283.
- [41] O. Hunderi, N. Ryum, The kinetics of normal grain growth, *J. Mat. Sci.* 15 (1980) 1104–1108.
- [42] A.D. Rollett, D.J. Srolovitz, M.P. Anderson, Simulation and theory of abnormal grain growth—anisotropic grain boundary energies and mobilities, *Acta Metall.* 37 (1989) 1227–1240.
- [43] G.I. Barenblatt, *Scaling, Self-similarity and Intermediate Asymptotics*, Cambridge University Press, New York, 1996.
- [44] J.L. Mason, E.A. Lazar, R.D. MacPherson, D.J. Srolovitz, Geometric and topological properties of the canonical grain-growth microstructure, *Phys. Rev. E* 92 (2015) 063308.
- [45] K. Barmak, M. Emelianenko, D. Golovaty, D. Kinderlehrer, S. Ta'asan, Towards a statistical theory of texture evolution in polycrystals, *SIAM J. Sci. Comput.* 30 (6) (2008) 3150–3169.
- [46] K. Barmak, E. Eggeling, M. Emelianenko, Y. Epshteyn, D. Kinderlehrer, R. Sharp, S. Ta'asan, Critical events, entropy, and the grain boundary character distribution, *Phys. Rev. B* 83 (2011) 134117, <http://dx.doi.org/10.1103/PhysRevB.83.134117>.
- [47] E.A. Lazar, R. Pemantle, Coarsening in one dimension: invariant and asymptotic states, *Israel J. Math.* (2015) (in press). arXiv:1505.07893v2 [mathPR].